Tape Casting of High Dielectric Ceramic Substrates for Microelectronics Packaging

A.I.Y. Tok, F.Y.C. Boey, and M.K.A. Khor

(Submitted 28 September 1998; in revised form 25 January 1999)

The production of ceramic green tapes is integral to the production of multilayer ceramic packages and capacitors. This article presents a batch type process for producing alumina ceramic green tape down to 150 μm thickness. The process parameters relevant to the precise control of the thickness of an alumina-based ceramic tape have been investigated using a float glass tape caster. Results indicate that the cast tape thickness was dependent on the blade gap until it reached a limiting value. This limiting thickness in turn was dependent on the casting speed, with a higher speed producing thinner tapes. Optimal casting was shown to exist when the blade gap was set at or beyond the limiting value, with the casting speed the controlling factor for the final thickness.

Keywords alumina, ceramics tape cast, tape thickness

1. Introduction

The trend in the microelectronics packaging industry toward greater densification, miniaturization, and higher computing speeds has imposed increasing demands on materials for higher thermal properties, better dielectric strength, and improved reliability, leading to the increased usage of ceramics in the form of multilayer substrates, for example in pin grid array (PGA) and ball grid array (BGA) applications. Current usage of high performance systems such as high purity alumina substrates has resulted in the use of thinner substrates. The production of such ceramic substrates is the subject of this article.

Currently, one of the main methods used for the manufacture of flat ceramic substrates with precisely controlled thickness and consistency is the tape casting technique. This method basically starts with a specially formulated slurry, which can be cast by a blade to a flat sheet or layer, then dried into a flexible solid tape, which can be sintered subsequently into a hard ceramic substrate layer. The applications of tape casting include Al_2O_3 and AlN substrates for thin and thick film circuitry (Ref 1), piezoelectric ceramics for actuators (Ref 2), photovoltaic solar cells (silicon-on-ceramics, or SOC) using mullite tape cast substrates (Ref 3), and others (Ref 4).

A customized tape caster with a special pressure control unit has been developed that is able to produce thin but consistent and very flat substrates for this project. Current research work is comprehensively separated into three areas: material and process formulation for a composite slurry based on alumina/aluminum nitride, development of a control system and a process model to produce required tape cast sheets with the required dimensional accuracy and consistency, and finally development of an optimal debinding and sintering process for the final composite multilayered substrates.

A.I.Y. Tok, F.Y.C. Boey, and **M.K.A. Khor,** School of Mechanical and Production Engineering, Nanyang Technological University, Singapore. Contact e-mail: mkakhor@ntu.edu.sg.

In the tape casting process, ceramic particles and other essential additives are dispersed in a solvent to form a slurry. The slurry is layered onto a carrier by passing it under a doctor blade of preset gap either onto a moving carrier (Fig. 1) or onto a fixed casting surface using a traversing casting head. The slurry is then allowed to dry, and a thin ceramic green tape is formed. After drying, a high concentration of organic components remain in the tape, which must be removed by pyrolysis. This burning out of organic compounds generates an open porosity in the green tape, which must be eliminated by sintering, a high diffusion process.

The control of green tape thickness is crucial in governing the properties of the tape cast products. Currently, the production and accurate reproduction of smaller and thinner substrates are limited by several factors, one of which is the precise control of the green tape thickness. This is in turn influenced by the various processing parameters and formulation of the materials used.

Theoretical modeling of the flow characteristics has been used to predict the green tape thickness after casting. Chou et al. (Ref 5) analyzed the tape casting flow behavior using the principles of fluid dynamics. They assumed a Newtonian flow for the slurry in a parallel channel consisting of both a Couette and Poiseuille flow and obtained the following equation:

$$\delta_{tape} = \frac{\alpha\beta}{2}\frac{\rho\, h_o}{\rho_{tape}}\left(1 + \frac{h_o^2\,\Delta P}{6\eta UL}\right) \quad \text{(Eq 1)}$$

where

α is side flow correction factor
β is shrinkage correction factor
δ_{tape} is tape thickness
ρ is slurry density, kg/m^3
ρ_{tape} is tape density, kg/m^3
h_o is doctor blade gap height, mm
η is slurry viscosity, Pa · s
L is doctor blade channel length, mm
ΔP is slurry pressure head, Pa
U is casting speed, mm/s

Equation 1 basically indicates a polynomial relationship between the tape thickness, δ_{tape}, and the blade gap, h_o. A decrease or an increase in the blade gap can be effected linearly by changing the slurry pressure head, ΔP, or the casting speed.

Other attempts at modeling tape casting flow behavior include work by Ring (Ref 6), who used the Bingham constitutive equation for a non-Newtonian slurry, and Huang et al. (Ref 7), who assume the slurry behaves according to the Herschel-Bulkley model.

2. Experimental Procedure

Figure 2 summarizes the overall process steps for producing the tapes. The tape casting was performed using the formulation listed in Table 1. A dual solvent system of trichloroethylene (C_2HCl_3) and ethanol (C_2H_6O) was chosen to improve organic solubility and prevent preferential volatilization and polymeric surface skin formation.

The sequence of component addition affected the viscosity of the slurry, due to preferential adsorption and water adsorption effects (Ref 8, 9). It was critical that the deflocculant be introduced independent of the other polymers to prevent competition for adsorption sites on the ceramic particulate surface and therefore produce more uniform slurry viscosities (Ref 10). The plasticizer was added to the slurry before the binder to aid the dissolution of the binder into the overall slurry, due to the preferred solubility of the binder in the plasticizer relative to the solvent system.

The alumina powder (98% extra pure, 5 to 15 μm) was mixed with a compatible sintering aid, magnesium oxide (98% extra pure), and ball milled at 60 rpm for 24 h in a 1 L corundum milling jar with high-purity aluminum oxide ball charges. The ball-to-weight ratio used was 15 to 1. After ball milling, the deflocculant and solvents were added to the mixed powders to form a slurry. This slurry was then placed in an ultrasonic bath and ultrasonically agitated for 45 min at 47 kHz (35 W). Sequential addition of plasticizer and binder to the slurry was performed after ultrasonic deagglomeration, and the slurry was mechanically mixed for 2 h to dissolve the organic additives in the solvents and to achieve a homogeneous mix.

After mixing was complete, the homogenous slurry was then transferred to a vacuum chamber where it was deaired at 700 mm Hg (90 kPa) for 20 min. The slurry was then sieved with two nylon sieves with openings 0.032 and 0.020 mm to remove any remaining agglomerates, aggregates, milling debris, and contaminants.

Tape casting was performed on a batch process type caster, where the casting head and doctor blade traversed over a stationary floating glass slab, discharging slurry onto the surface. The doctor blade gap was varied by a micrometer screw gauge,

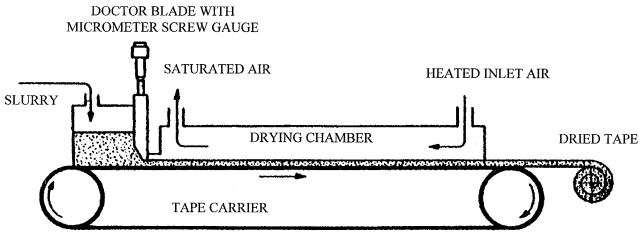

Fig. 1 A continuous tape casting machine

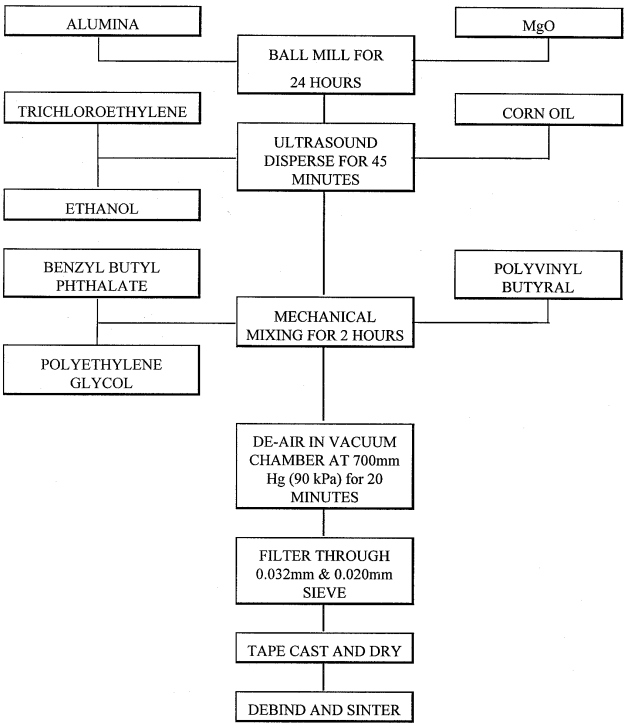

Fig. 2 Tape casting process flowchart

Table 1 Tape casting formulation

Component	Function
Aluminum oxide	Ceramic substrate
Magnesium oxide	Grain growth inhibitor
Trichloroethylene	Solvent
Ethanol	Solvent
Corn oil	Deflocculant
Polyethylene glycol	Plasticizer
Benzyl butyl phthalate	Plasticizer
Polyvinyl butyral	Binder

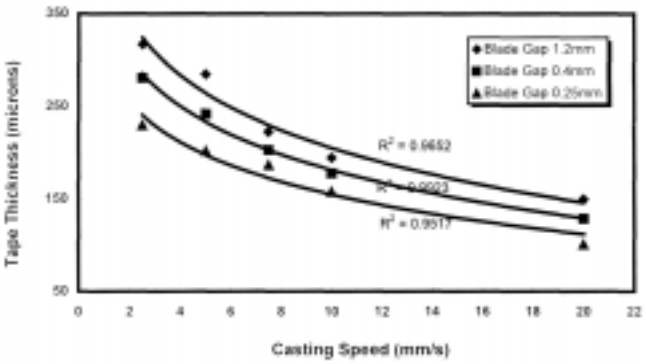

Fig. 3 Plot of the green tape thickness obtained at different casting speeds for three different blade gaps showing a logarithmic regressed trend

with an accuracy of up to 10 μm. Accurate casting velocity control was achieved via a personal computer (PC) based stepping motor. The cast tape thickness was accurately measured by sandwiching the tape between two pieces of thin glass of known thickness and using a micrometer to measure the total thickness. This method of measurement eased pressure from the micrometer jaws, which might cause that small portion of tape to compress and provide inaccurate results.

3. Results and Discussion

Figure 3 plots the tape thickness obtained as the casting speed was changed for three different blade gaps. The thickness was seen to decrease exponentially with increases in the casting speed for all three blade gaps. This change in the blade gaps did not result in a proportional change in the tape thickness, as shown more clearly when the thickness is plotted against the blade gap in Fig. 4, which indicates a maximum achievable thickness for a given casting speed. The tape thickness increased at very small blade gaps but leveled off to a constant thickness past a certain blade gap value. The limiting blade gap was smaller for faster casting speeds (Fig. 5).

The previously mentioned results highlight the difficulty involved in achieving consistent tape thickness. As shown in Fig. 6, the desired tape thickness required should ideally be obtained when the thickness becomes independent of the blade gap and depends only on the casting speed. Figure 5 also shows that a faster casting speed will lower the tape thickness obtainable. However, it would appear that there is a limiting thickness that can be achieved, even at very fast casting speed for a given pressure and slurry viscosity.

The results obtained have been compared to the model developed by Chou et al. (Ref 5), indicated in Eq 1 and shown in Fig. 7. There was a good correlation between the experimental and predicted values only above a blade gap of 400 μm. Below this blade gap value, the predicted thickness was actually higher than the blade gap setting, which is impossible.

One reason for this discrepancy was the assumption made in the model that the slurry was a Newtonian fluid. Figures 8 to 10 show the results of the measured viscosity of the tape casting slurry, using a controlled rate rheometer. Two different measurements were made: one of the complete processed slurry and one of the mixed polymeric liquid media alone. The latter behaved as a Newtonian fluid, with the viscosity being independent of the shear rate (Fig. 8). However, the slurry showed a shear thinning behavior indicative of a non-Newtonian shear thinning fluid (Fig. 9).

Figure 10 compares the results for the slurry to an Ostwald de Waele (power-law) shear thinning model, where the shear stress tends to zero at zero shear rate:

$$\sigma = K\dot{\gamma}^n \quad \text{(Eq 2)}$$

where σ is shear stress, Pa, and $\dot{\gamma}$ is strain rate, 1/s. The results indicate a good fit, with the coefficient of determination, R^2, giving a very high 0.996 value, with the regressed value of the power exponent $n = 0.675$. It is worthy to note that the Herschel-Bulkley model (Ref 11) is actually an extension of the Ostwald de Waele model in that a yield stress, σ_y, is added:

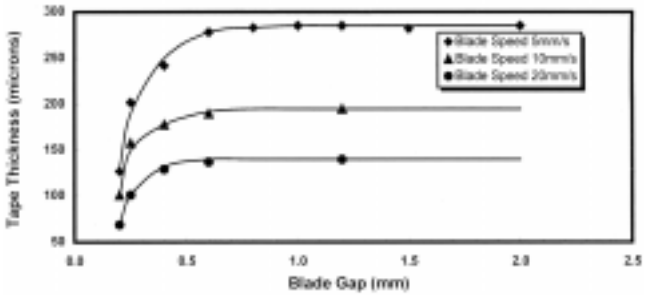

Fig. 4 Plot of the green tape thickness obtained at different blade gaps for three different casting speeds

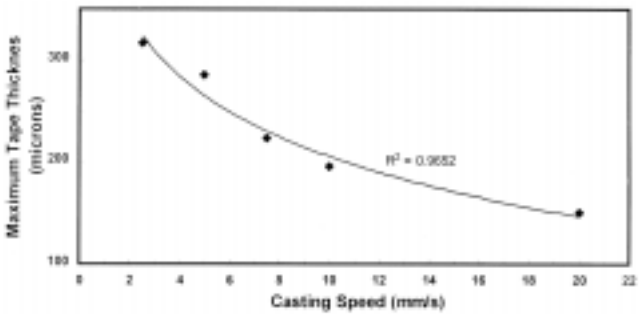

Fig. 5 Plot of the maximum green tape thickness obtained at different casting speeds showing a logarithmic regressed trend

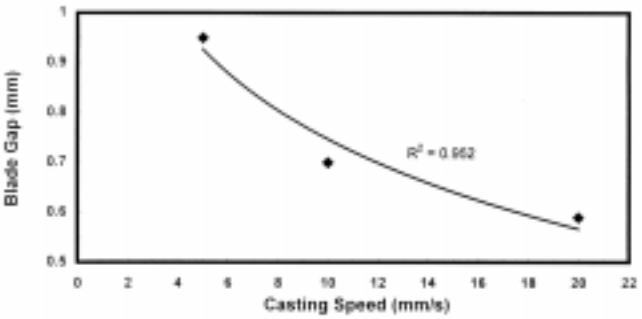

Fig. 6 Plot of the blade gap setting at which the maximum green tape thickness occurs for different casting speeds showing a logarithmic regressed trend

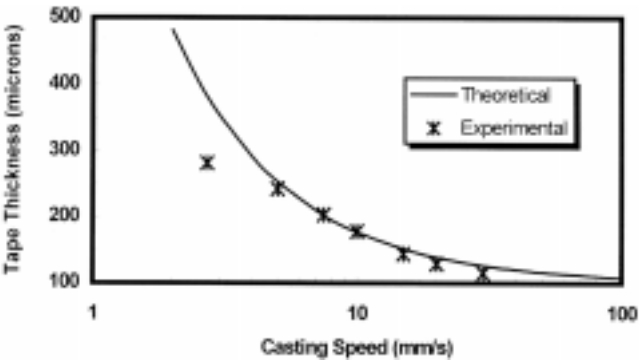

Fig. 7 Plot of experimental results vs. theoretical predictions (Chou et al., Ref 5)

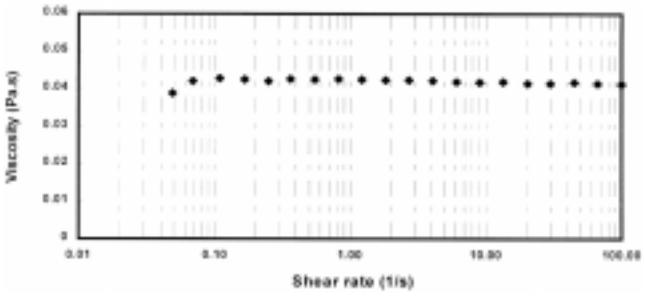

Fig. 8 Plot of the polymeric liquid media viscosity at varying shear rates

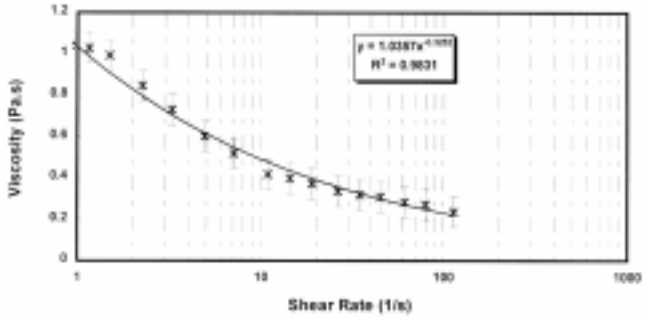

Fig. 9 Plot of slurry viscosity at varying shear rates

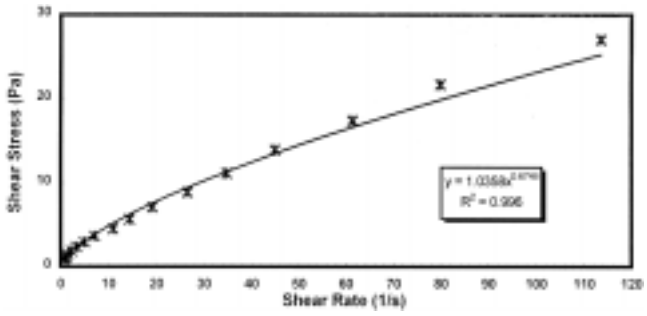

Fig. 10 Plot of slurry shear stress vs. shear rate

$$\sigma = \sigma_y + K\gamma^n \quad \text{(Eq 3)}$$

The model by Chou et al. (Ref 5) also included two correction factors: side flow correction factor, α, and tape shrinkage during drying, β. In practice, the degree of side flow varied with changes in casting speed and blade gap setting. Changes in viscosity would therefore also affect the degree of shrinkage and side flow. It would also be very difficult to measure the thickness of the freshly cast tape unless sophisticated optical methods were used. Also the tape might already start to shrink (dry) before the thickness measurement.

4. Conclusions

From the results, it can be concluded that a higher degree of accuracy in tape thickness can be obtained when casting at lower casting speeds. However, this accuracy decreases when thinner tapes are required, and the optimized use of an increased casting speed would be needed to maintain this accuracy.

An optimal setting between the casting speed and the blade height setting is therefore needed in order to achieve accurate and reproducible results when performing tape casting. Determination of this optimum combination depends on the required thickness of the final product.

Because the slurry behaves according to Ostwald de Waele (power-law) shear thinning model, this reduces theoretical modeling parameters because the power-law model is in itself a simple mathematical model.

References

1. G. Fischer, Electronic Products Weathering Market Swings, *Am. Ceram. Soc. Bull.*, Vol 66, 1987, p 636
2. S. Takahashi, Longitudinal Mode Multilayer Piezoelectric Actuators, *Am. Ceram. Soc. Bull.*, Vol 65, 1986, p 1156-1159
3. C. Fiori and G. De Portu, Tape Casting: A Technique for Preparing and Studying New Materials, *Br. Ceram. Proc.*, Vol 38, 1986, p 213-225
4. A.I.Y. Tok, F.Y.C. Boey, and M.K.A. Khor, "Tape Casting of High Dielectric Ceramics Composite/Hybrid Substrates for Microelectronics Application," Proceedings of the 6th International Conference on Processing and Fabrication of Advanced Materials (Singapore), 1997
5. Y. Chou, Y. Ko, and M. Yan, Fluid Flow Model for Ceramic Tape Casting, *J. Am. Ceram. Soc.*, Vol 70 (No. 10), 1987, p C280-282
6. T.A. Ring, A Model of Tape Casting Bingham Plastic and Newtonian Fluids, *Adv. Ceram.*, Vol 26, M.F. Yan, Ed., American Ceramic Society, 1989, p 569-576
7. X.Y. Huang, C.Y. Liu, and H.Q. Gong, A Viscoplastic Flow Modeling of Ceramic Tape Casting, *Mater. Manuf. Process.*, Vol 12 (No. 5), 1997
8. W.R. Cannon, R. Becker, and K.R. Mikeska, Interactions among Organic Additives Used for Tapecasting, *Adv. Ceram.*, Vol 26, M.F. Yan, Ed., American Ceramic Society, 1989, p 525-541
9. D.J. Shanefield, Competing Adsorptions in Tape Casting, *Adv. Ceram.*, Vol 19, M.F. Yan, Ed., American Ceramic Society, 1988, p 155-160
10. L. Braun, J.R. Morris, Jr., and W.R. Cannon, Viscosity of Tape-Casting Slips, *Am. Ceram. Soc. Bull.*, Vol 64 (No. 5), 1985, p 727-729
11. W.H. Herschel and R. Bulkley, *Proceedings of ASTM, Part II*, Vol 26, 1926, p 621-629